Surface stress on the erythrocyte under laser irradiation with finite-difference time-domain calculation

Ji-Tong Yu
Ji-Yao Chen
Zhi-Fang Lin
Fudan University
Department of Physics
Shanghai 200433, China
E-mail: jychen@fudan.edu.cn

Lei Xu
Pei-Nan Wang
Fudan University
State Key Laboratory for Advanced Photonic Materials and Devices
Shanghai 200433, China

Min Gu
Swinburne University of Technology
Centre for Micro-Photonics
Faculty of Engineering and Industrial Sciences
PO Box 218 Hawthorn
Victoria 3122, Australia

Abstract. The surface stress on the real shape (biconcave disklike) of an erythrocyte under laser irradiation is theoretically studied according to the finite-difference time-domain (FDTD) method. The distribution of the surface stresses depends on the orientation of erythrocytes in the laser beam. Typically when the erythrocyte was irradiated from the side direction (the laser beam was perpendicular to the normal of the erythrocyte plane), the surface stresses were so asymmetrical and nonuniform that the magnitude of the surface stress on the back surface was three times higher than that on the front surface, and the highest-to-lowest ratio of the stress reached 16 times. For comparison, the surface stress was also calculated according to the ray optics (RO) method. The tendency of the stress distribution from the RO calculation was roughly similar to that of the FDTD method. However the RO calculation produced some unphysical results, such as the infinite stress on some surface region and the zero stress on the most parts of the erythrocyte surface, which is due to the neglecting of light diffraction. The results obtained from the FDTD calculation are believed quantitatively reliable, because the FDTD method automatically takes into account of the diffraction and interference effects of the light wave. Thus, the FDTD method is more suitable than the RO method for the stress study of erythrocytes. [DOI: 10.1117/1.2136847]

Keywords: erythrocyte; laser irradiation; stress; finite difference time domain.

Paper 05065RR received Mar. 8, 2005; revised manuscript received Jul. 7, 2005; accepted for publication Jul. 15, 2005; published online Dec. 8, 2005.

1 Introduction

The last two decades have witnessed many applications of lasers in biomedical fields.[1,2] Among others, a notable event is laser trapping, which can manipulate biological cells in a nontouch way by a laser beam.[3,4] The principle is that a net force is exerted on the whole object such as a cell through a total momentum transfer from a laser beam. The momentum transfer actually occurs on the surface of the object.[5] Furthermore, it has been found that the local forces on the object surface are much larger than the total net forces under laser irradiation,[6] and this surface stress is always perpendicular to the interface between the two media with the direction pointing to the medium of a lower refractive index.[7] Therefore, the object will experience the stretching forces under laser irradiation when surrounded by a medium with a lower refractive index. Such stretching forces can be used to measure the viscoelastic properties of the elastic object, especially the viscoelasticity of the membrane of living cells.[8] Consequently, an optical device called an optical stretcher was designed and the osmotically swollen spherical erythrocytes were successfully stretched.[6] Meanwhile, the surface stress theoretically calculated by the ray optics (RO) method was consistent with the experimental observation.[6] The optical stretching work revealed an important phenomenon that the erythrocyte could be stretched under laser irradiation. Such a stretched deformation may help improve the deformability of erythrocytes.

Low-power laser irradiation has been used in various medical researches as well as clinical applications.[9–12] We have found from the previous work that laser irradiation can improve the erythrocyte deformability;[13] however, the mechanism is not clear. The stretching forces on erythrocytes may be involved in the mechanisms of the erythrocyte deformability under laser irradiation. Although this work studied the surface stress in experiment as well as the theoretical calculation,[6] the erythrocyte shape used in their calculation was a swollen erythrocyte with a spherical shape. However, under the physiological conditions, erythrocytes appear in a biconcave disklike shape. The effect on erythrocytes with a real shape under laser irradiation is of great interest. In this paper, the surface stress on the real shape of an erythrocyte in the blood plasma was calculated by the finite-difference time-domain (FDTD) method. Although most work in this aspect has been done by the RO method, the RO method is only an approximate method due to the negligence of the diffraction effect. For a real shaped erythrocyte, the maximum thickness of the cell is only about 2.6 μm, while the wavelengths of

Address all correspondence to Ji-Yao Chen, Physics Dept., Fudan University, Handan Road 220, Shanghai 200433, China. Tel: 086–21–65642366. Fax: 086–2165104949. E-mail: jychen@fudan.edu.cn

1083-3668/2005/10(6)/064013/6/$22.00 © 2005 SPIE

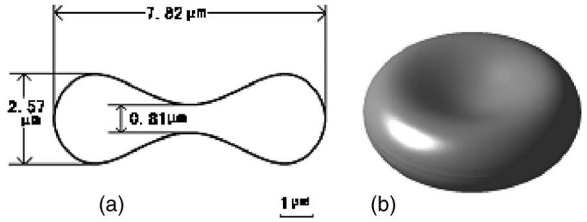

Fig. 1 (a) Vertical section and (b) the 3-D shape of the modeling of an erythrocyte.

lasers frequently used are in the region of 600 to 1000 nm (0.6 to 1 μm). Therefore, in such a real case, the effect of diffraction plays an important role and the RO method is not an ideal method of calculation. The FDTD method, on the other hand, is a convenient method developed to simulate electromagnetic waves in complex boundary conditions.[14–17] As a result, we have implemented the FDTD method, for the first time, to treat the surface stress problem of erythrocytes of a real biconcave disklike shape. By calculating the electric field distribution with the FDTD method, the surface stress can be obtained from the Maxwell stress tensor on the surface of an erythrocyte. For comparison, the RO method was also applied to calculate the surface stress for a real shaped erythrocyte.

2 Modeling an Erythrocyte and Measurement of the Refractive Indices

The modeling of the shape of erythrocytes follows the measurement results of Evans and Fung.[18] Figure 1 shows the biconcave shape of an erythrocyte with details of its geometry.

To calculate the surface stress, the refractive indices of the media inside and outside of the erythrocyte should be known first. A prism coupling apparatus was used to measure the refractive indices according to the critical angle of total reflection. The experimental setup is shown in Fig. 2. The liquid sample was pressed on the bottom plane of the prism with a small liquid vessel. A fixed incident laser beam (632.8 nm) travels into the prism and hits the bottom of the prism. The incident angle of the laser beam changes when a stepping motor rotates the prism. Light reflected from the bottom plane of the prism is detected. Total reflection occurs when the incident angle of the laser beam exceeds the critical angle of total internal reflection. By measuring the critical angle, the refractive index of the sample is determined. The smallest step of this stepping motor is 0.002 deg; the uncertainty of prism angle is 0.02 deg. Considering these two factors and the measuring error of the critical angle, the resolution of the refractive index measurement of this apparatus is less than 0.001.

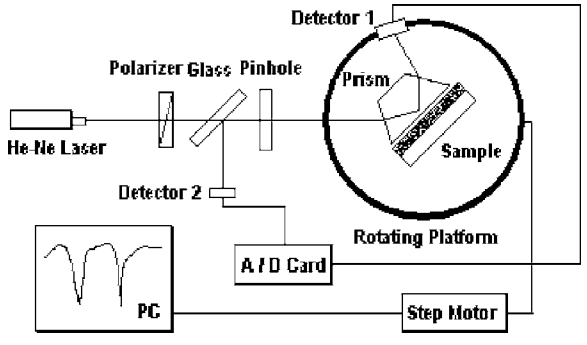

Fig. 2 Schematic of the experimental setup for the measurement of refractive indices.

The human blood was obtained from healthy volunteers. Centrifugation separated the erythrocytes and plasm. Then the packed erythrocytes (100% hematocrit) were centrifuged again with a superhigh speed (15,000 cycles/min) to break the membranes of the erythrocytes. After such centrifugation, the ghosts were gathered on the bottom of the centrifuging tube and the supernate was the hemoglobin cytoplasm of erythrocytes. Taking the supernate from the tube, we obtained the hemoglobin cytoplasm. The ideal hemoglobin cytoplasm can be obtained from the 100% hematocrit erythrocytes. However, in the course of erythrocyte packing and collecting, a departure from the 100% hematocrit exists and causes a concentration difference of hemoglobin cytoplasm, resulting in an error in the measurement of refractive indices. Through repeating the measurement, it was found this error was 0.001 under our conditions.

The refractive indices of the hemoglobin cytoplasm and the blood plasm were measured to be 1.380 and 1.351, respectively, at a wavelength of 632.8 nm. Since the refractive index of the blood plasm is smaller than that of the cytoplasm of erythrocytes, stretching forces will be exerted on erythrocyte surfaces when they are irradiated by a laser beam. To calculate this surface stress as well as its distribution on an erythrocyte, the power density of laser irradiation should be selected. In intravenous low-power laser irradiation for clinical use, a 5-mW 632.8-nm laser is introduced through a 100-μm-diam fiber injection. At the tip of the fiber in a vein, the power density is about 6.36×10^5 w/m^2. This power density was used in the following calculation, and the irradiation beam was approximated as a plane wave, which is appropriate in our case since the scattering erythrocyte is much smaller compared with the beam width.

3 RO Calculation

3.1 *Theory*

The momentum of a ray of light with energy E traveling in a medium with refractive index n is[5] nE/c (c is the speed of light in vacuum). The stress on the boundary surface can be calculated by the conservation of the momentum of light.[8] When a beam of light with a power density I hits the boundary of two materials with different refractive indices n_1 and n_2, the surface stress $\boldsymbol{\sigma}$ is given by[6]

$$\boldsymbol{\sigma} = (n_1/c)I\cos\alpha[(1+R)\cos\alpha - (n_2/n_1)(1-R)\cos\beta]\mathbf{n}, \tag{1}$$

where α and β denote the incident and the refractive angles, $\mathbf{n}$ is the unit normal pointing from medium 1 (n_1) to medium 2 (n_2), and R is the reflectivity. From Eq. (1), we can see that the direction of the stress is perpendicular to the surface and its magnitude is determined by two factors: the power density and the incident angle of the light beam.

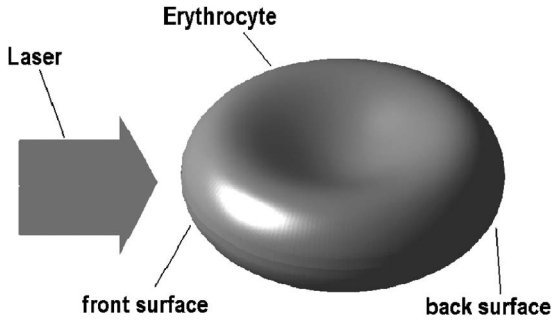

Fig. 3 Laser beam perpendicular to the normal of the erythrocyte plane.

3.2 *RO Treatment for Erythrocytes*

The incident laser beam reaches the surface of the erythrocyte area was divided into 16,000 rays, and each ray was traced when it passed into and out of the erythrocyte. This approach was similar to that of the previous work.[19] The sectional area of the light beam surrounded by every four neighboring rays was calculated to derive the power density of the light in different places on the surface of the erythrocyte. Then the surface stress was calculated using Eq. (1).

3.3 *Results*

3.3.1 *Side irradiation*

First, we calculated the surface stress on the erythrocyte when the laser beam irradiated the erythrocyte from the side direction, as shown in Fig. 3.

Figure 4 shows the calculation results for the surface stress on the erythrocyte with different viewing angles in this situation. The relative blackness represents the magnitude of the stress. The typical characteristic of the distribution of the surface stress is that it is quite nonuniform. The stress distribution can be divided into four main regions (regions A, B, C, and D). For most of the erythrocyte surface (region D), the stress is almost zero, with the very light blackness. On the front surface of the erythrocyte (region A), the stress is also low (about 6×10^{-5} N/m^2) with a light blackness, while at the back surface (region C) and in region B, the stress is much stronger (2.5×10^{-4} N/m^2) than that in the former two regions (regions A and D). The deep blackness at the edges of both regions B and C demonstrates that these areas experience

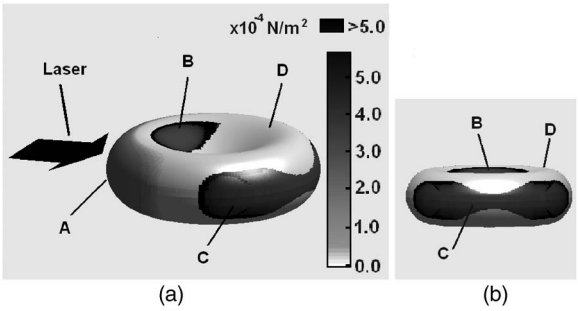

Fig. 4 Surface stress on the erythrocyte with the RO calculation, where (a) shows the distribution viewed from the direction opposite to the laser beam.

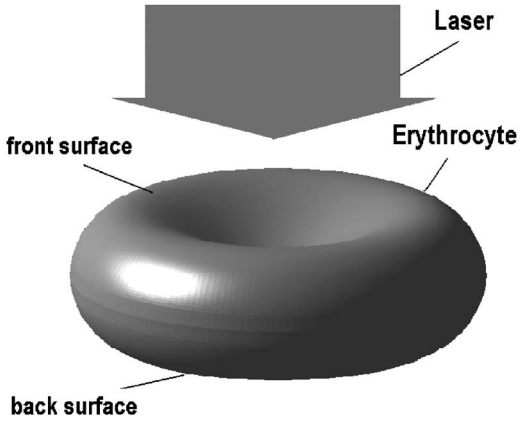

Fig. 5 Laser beam parallel to the normal of the erythrocyte plane.

the strongest stress. The strong stress (over 5×10^{-4} N/m^2) is due to the focusing effect and the total internal reflection on some of region B. In the middle of each deep blackness region, are lines where the stress approaches infinity. These lines are the focused lines where the rays intersect. Of course, the infinite stress would not exist in a real situation.

Another unreasonable phenomenon is that the highest stress region is just close to the lowest stress (zero) region. Such an unphysical result is due to neglecting the diffraction effect in the RO method. Here, in such a small area (about 10^{-4} μm for each ray) and considering the wavelength used (about 1 μm), the diffraction should be prominent during the light propagation through an erythrocyte. Thus, the RO method is not an ideal method to appropriately calculate the stress on the surface of an erythrocyte.

3.3.2 *Front irradiation*

In the other case, when the laser beam irradiated the erythrocyte from the front direction, as shown in Fig. 5, it was an axially symmetric case. The stress can be calculated as a function of the radius for the front surface and the back surface, respectively. Figure 6 shows the calculation results for the front surface (a) as well as the back surface (b) of the erythrocyte by the RO method, where the thick lines and the dotted lines represent the surfaces of the erythrocyte and the thin lines demonstrate the stress distribution on both surfaces.

Unlike the case of side irradiation, a uniform characteristic of the stress distribution appears on most parts of the front surface of the erythrocyte and the magnitude of the stress is similar (about 6×10^{-5} N/m^2) except for the value on the edge of erythrocyte where the magnitude of the stress decreases rapidly. The stress distribution on the back surface is shown in the Fig. 6(b). On most parts of the back surface, the stress distribution is still uniform with the similar magnitude but the stress slightly increases from the center to the edge. The magnitude of the stress is close to that on the front surface (about 6×10^{-5} N/m^2). However, at the edge of the back surface, the stress increases dramatically. In this case, the front surface behaves just like a lens, focusing the laser beam and resulting in the strongest stress. The scope of the edge part of the erythrocyte is only a few microns, so the negli-

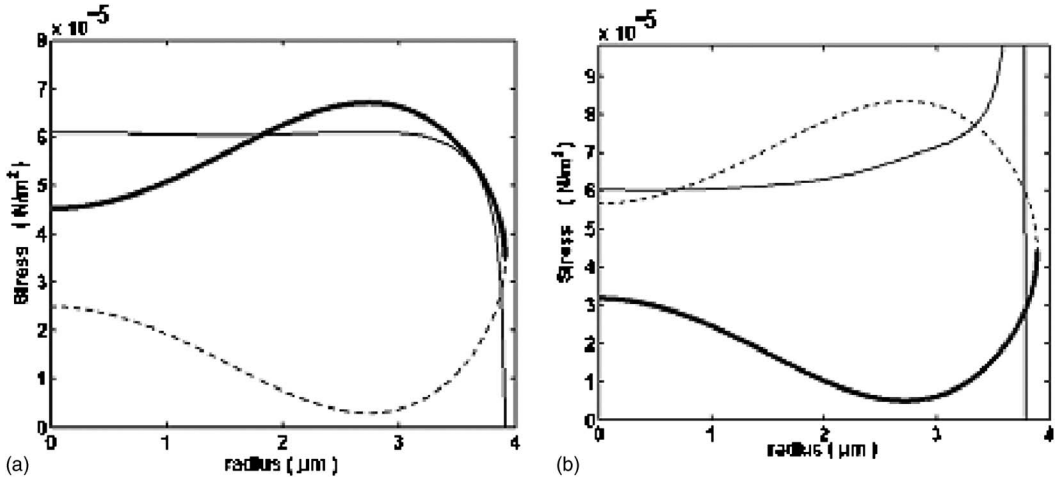

Fig. 6 Stress on (a) the front surface and (b) the back surface of erythrocyte with the RO calculation. The thick lines represent the front surface in (a) and the back surface in (b). The dotted lines represent the back surface in (a) and the front surface in (b). The thin lines show the stress distribution versus the erythrocyte radius.

gence of the diffraction effect is also not reasonable. It can be predicted that the strongest stress on the edge will be lowered when the diffraction is considered.

4 FDTD Calculation

4.1 *Theory*

The components of the Maxwell stress tensor ($\mathbf{T}$) in the dielectric medium can be written as[20,21]

$$T_{ij} = \varepsilon\left[E_i E_j + \frac{1}{\varepsilon\mu} B_i B_j - \frac{1}{2}\left(\mathbf{E}\cdot\mathbf{E} + \frac{1}{\varepsilon\mu}\mathbf{B}\cdot\mathbf{B}\right)\delta_{ij}\right]$$

$$= D_i E_j + H_i B_j - \frac{1}{2}(\mathbf{D}\cdot\mathbf{E} + \mathbf{H}\cdot\mathbf{B})\,\delta_{ij}, \tag{2}$$

where ε and μ are the electric permittivity and magnetic permeability of the dielectric medium, $\mathbf{E}$ and $\mathbf{B}$ are the electric field and the magnetic induction, $\mathbf{D}=\varepsilon\mathbf{E}$ and $\mathbf{H}=\mathbf{B}/\mu$ are the electric displacement and magnetic field, and the δ_{ij} is the delta function (its value becomes 1 only when i equals j).

On the boundary of two media (1 and 2), the ith component of the surface stress is[21]

$$\sigma_i = \sum_j (T_{2_{ij}} - T_{1_{ij}}) n_j. \tag{3}$$

Here $\mathbf{n}$ is the normal of the surface pointing from medium 1 to medium 2, and the n_j is the component of the $\mathbf{n}$. Using the boundary conditions at the surface, we can express the stress as[7]

$$\boldsymbol{\sigma} = \frac{1}{2}[(\varepsilon_1 - \varepsilon_2)E_t^2 - (\varepsilon_1 E_{1n}^2 - \varepsilon_2 E_{2n}^2)]\mathbf{n}. \tag{4}$$

Here E_{1n} and E_{2n} are the components of the electric fields perpendicular to the surface in media 1 and 2, E_t is the component of the electric field parallel to a surface that is continuous across the surface. Using the boundary conditions for E_{1n} and E_{2n}:

$$\varepsilon_1 E_{1n} = \varepsilon_2 E_{2n},$$

Eq. (4) can be expressed as

$$\boldsymbol{\sigma} = \frac{1}{2}(\varepsilon_1 - \varepsilon_2)(E_t^2 + E_{1n}E_{2n})\mathbf{n}. \tag{5}$$

If we introduce an averaged electric field $\bar{\mathbf{E}}$ on the surface, the components of which defined as:

$$\bar{E}_t = E_{1t} = E_{2t},$$

$$\bar{E}_n = (E_{1n}E_{2n})^{1/2} = (\varepsilon_1/\varepsilon_2)^{1/2}E_{1n} = (\varepsilon_2/\varepsilon_1)^{1/2}E_{2n}, \tag{6}$$

then the stress is simplified as

$$\boldsymbol{\sigma} = \tfrac{1}{2}(\varepsilon_1 - \varepsilon_2)\bar{E}^2\mathbf{n}. \tag{7}$$

The new expression makes the stress $\boldsymbol{\sigma}$ easier to be understood. The stress $\boldsymbol{\sigma}$ is determined by two terms, the difference between the permittivities of two materials and the averaged electric field on the surface. Since the refractive index is equal to the square root of permittivity ε, the first term is related to the difference of refractive indices in two media. In addition, this new expression also simplifies the FDTD calculation.

4.2 *Treatment for Erythrocyte*

The electric field distributions were calculated using the FDTD method, and then the surface stress could be obtained according to Eq. (7). The three-dimensional (3-D) calculation region consisted of $172\times172\times172$ meshes over the $10\times10\times10$ μm computing area, which means this area contains 172^3 small cubic boxes with the size of $0.058\times0.058\times0.058$ μm for each box. The erythrocyte was arranged in the center of the computing area. The hemoglobin cytoplasm inside erythrocyte was treated as homogeneous and the membrane of the erythrocyte was neglected. In the calculation, these small boxes inside the erythrocyte were set to have the refractive index of hemoglobin cytoplasm and the boxes out-

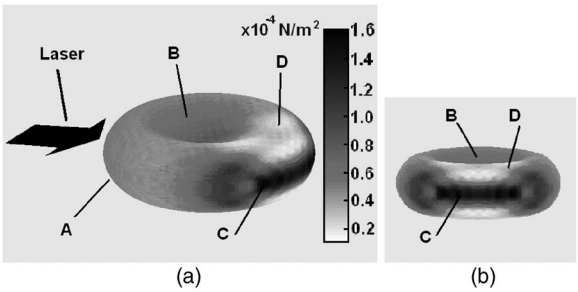

Fig. 7 Surface stress on the erythrocyte with the FDTD calculation. The right figure shows the distribution viewed from the direction opposite to the laser beam.

side erythrocyte have the refractive index of blood plasma. The erythrocyte had the biconcave disklike surface shape. Here the surface of erythrocyte was treated as the composing outline of those small cubic bricks (e.g., boxes) located on the erythrocyte surface. The outmost 10-mesh perfect match layer (PML) was set as the absorbing boundary, which is one of the standard treatments in the FDTD method.[22] The temporal step size Δt was taken as 40 as. The total field/scattered field formulation was used to introduce the incident light. For simulating the incident light of a plan wave, the corresponding connecting conditions[23] were set on the surrounding grids of the erythrocyte. The details of this formulation can be found in Ref. 23 and 24.

4.3 *Results*

4.3.1 *Side irradiation*

In this case, the erythrocyte was irradiated from the side direction, as shown in Fig. 3. The distribution of the surface stress from the FDTD calculation is demonstrated in Fig. 7. Such a stress distribution is qualitatively in agreement with that obtained from the RO calculation. That is, the stress with the highest value appears in region C (back surface) and lowers its magnitude in region B, the magnitude of the stress is even lower in region A (front surface), and finally the stress turns to lowest in region D. However, the difference between the results from the two calculations is obvious. The FDTD method is based on the direct implementation of Maxwell's time-dependent curl equations. In this way, the light beam is treated as an electromagnetic wave and the effect of diffraction is automatically included in the treatment. Thus, on the whole surface of the erythrocyte, no region of the zero and infinite stress appears, which is quite reasonable from the view point of diffraction. In addition, the FDTD method provides the reasonable quantitative data of the surface stress, which is 1.4×10^{-4} N/m^2 in the central area of the region C, 1.0×10^{-4} N/m^2 in the surrounding areas of the region C, 0.6×10^{-4} N/m^2 in region A, and only 0.1×10^{-4} N/m^2 in region D, respectively. Although the ratio of the highest stress to the lowest stress reaches 16, the surface stress changes smoothly and continuously from one region to another, as seen in Fig. 7 from the deepest blackness area shifting to the deeper blackness area then to the light blackness area. In contrast, the stress from the RO calculation does not continuously change in the different regions of the surface. For example, the deepest blackness area is directly connected to the lightest blackness area, which implies a sudden drop of the stress from the highest value to the value of zero (Fig. 4).

Here the stress distribution on the real shape erythrocyte differs with that on the spherical erythrocyte in the previous report.[6] The stress on the back surface is three times higher than that on the front surface, and the ratio of the highest stress to the lowest stress reaches 16, while the difference of the stress between the back and front surfaces of the spherical erythrocyte was less than 10%.

4.3.2 *Front irradiation*

Figure 8 demonstrates the stress distribution from the FDTD calculation when the erythrocyte was irradiated from the front direction (as shown in Fig. 5). Generally, the magnitude of the stress on most parts of the surface is similar to that obtained from the RO calculation. However, there are two main differences of the results between the FDTD and RO methods. First, on the front surface, unlike the result in the RO method, the stress curve in Fig. 8(a) is not as flat; the fluctuation of the stress can clearly be seen. This stress fluctuation is a reason-

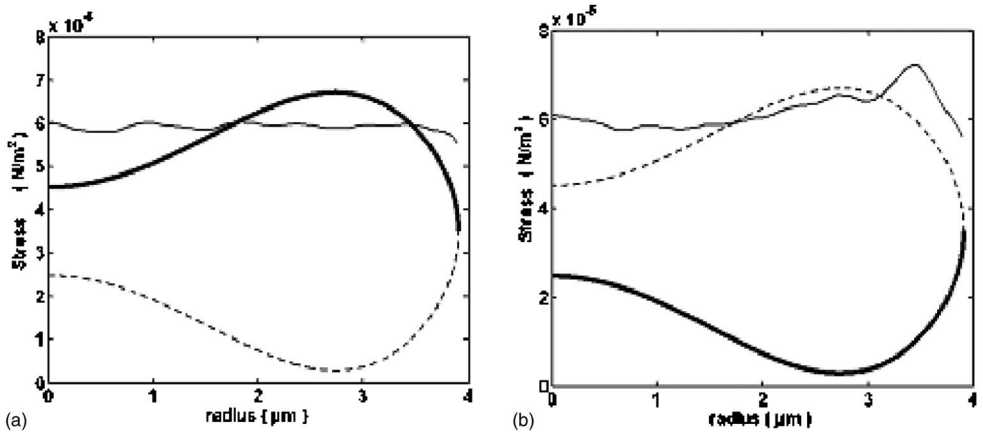

Fig. 8 Stress on (a) the front surface and (b) the back surface of erythrocyte with the FDTD calculation. The thick lines represent the front surface in (a) and the back surface in (b). The dotted lines represent the back surface in (a) and the front surface in (b). The thin lines show the stress distribution versus the erythrocyte radius.

able result due to the electromagnetic wave interference. The forward wave and the backward wave reflected from the back surface interferes, resulting in the undulation of **E** around the surface so as to the undulation of the stress. However, in the method of RO, the partial reflection from the back surface is totally neglected. Second, as shown in Fig. 8(b), though there is still a small peak of the stress at the edge of the erythrocyte, the steep changing of the stress in the RO method is passivated here. The diffraction abates the focusing effect as that in the RO treatment.

In the FDTD calculation, the smooth surface of a real erythrocyte was treated as the wrinkling boundary consisting of many interface-localized small cubic bricks, which results in an error. To estimate the error of the FDTD method, a comparison was made. The stress on the typical dielectric sphere with a size similar to the erythrocyte was calculated by the FDTD method with the same mesh arrangement as well as by the Mie theory. The Mie theory has been known as an accurate theory for the treatment of the propagation of an electromagnetic wave through spherical objects.[25] Taking the Mie results as the accurate solution and comparing it with the FDTD results, we found that the error of the FDTD calculation was about 4% here, depending on the meshes employed. If the more meshes are chosen in the FDTD treatment (which cost more calculation time), the error will decrease accordingly. Although the Mie theory is believed to be an accurate method, it can be applied only to an object with a spherical shape. For a complex boundary object, the Mie method is not useful, while the FDTD method is good at treating complex boundary objects, and although it is not perfect, it retains relatively good precision.

5 Conclusion

In the stress study of a real shaped erythrocyte, the RO method is not suitable, because the critical condition for the RO treatment (the ratio of the object dimension to the laser wavelength $\gg 1$) is not completely satisfied. The FDTD treatment, automatically taking into account the effects of diffraction and interference, supplies reliable results. It is evident that the FDTD method is a suitable way to treat complex boundary objects such as erythrocytes. With the FDTD calculation, it has been found that the surface stress on a real shaped erythrocyte is orientation dependent when the erythrocyte is irradiated by a laser beam. Under the condition of front irradiation, the stress varies appreciably (less than 15%) on the whole surface. In the case of side irradiation, the stress changes significantly so that the stress on the back surface is 3 times higher than that on the front surface, and the ratio between the highest stress area and the lowest stress area reaches 16.

Acknowledgments

This work was supported by the National Science Foundation of China (No. 10174017), the Shanghai Municipal Science and Technology Comission (04DZ05617), as well as Chun-Tsung scholar program.

References

1. E. Mester, A. F. Mester, and A. Mester, "The biomedical effects of laser application," *Lasers Surg. Med.* **5**, 31–39 (1985).
2. J. R. Basford, "Low intensity laser therapy: still not an established clinical tool," *Lasers Surg. Med.* **16**, 331–342 (1995).
3. A. Ashkin, J. M. Dziedzic, and T. Yamane, "Optical trapping and manipulation of single cells using infrared laser beams," *Nature (London)* **330**, 769–771 (1987).
4. S. C. Kuo and M. P. Sheetz, "Optical tweezers in cell biology," *Trends Cell Biol.* **2**, 116–118 (1992).
5. S. Chu, "Laser manipulation of atoms and particles," *Science* **253**, 861–866 (1991).
6. J. Guck, R. Ananthakrishnan, T. J. Moon, C. C. Cunningham, and J. Käs, "Optical deformability of soft biological dielectrics," *Phys. Rev. Lett.* **84**, 5451–5454 (2000).
7. K. Okamoto and S. Kawata, "Radiation force exerted on subwavelength particles near a nanoaperture," *Phys. Rev. Lett.* **83**, 4534–4537 (1999).
8. J. Guck, R. Ananthakrishnan, H. Mahmood, T. J. Moon, C. C. Cunningham, and J. Käs, "The optical stretcher: a novel laser tool to micromanipulate cells," *Biophys. J.* **81**, 767–784 (2001).
9. S. Halevy, R. Lubart, H. Reuveni, and N. Grossman, "780 nm low power laser therapy for wound healing in vivo and in vitro studies," *Laser Ther.* **9**, 159–164 (1997).
10. J. S. Surinchak, M. L. Alago, and R. F. Bellamy, "Effects of low-level energy lasers on the healing of full-thickness skin defects," *Lasers Surg. Med.* **2**, 267–274 (1983).
11. T. Lundeberg and M. Malm, "Low power He–Ne laser treatment of venous leg ulcers," *Ann. Plast. Surg.* **27**, 537–539 (1991).
12. N. Kipshidze, H. Sahota, H. Wolinsky, R. Komorowski, L. E. Boerboom, S. D. Keane, M. H. Keelan, and J. E. Baker, "Photoremodeling of the atherosclerotic arterial wall inhibits myointimal hyperplasia following balloon angioplasty," *Circulation* **90**, 332 (1994).
13. X. Q. Mi, J. Y. Chen, Y. Cen, Z. J. Liang, and L. W. Zhou, "A comparative study of 632.8 and 532 nm laser irradiation on some rheological factors in human blood in vitro," *J. Photochem. Photobiol., B* **74**, 7–12 (2004).
14. K. S. Yee, "Numerical solution of initial boundary value problems involving Maxwell's equations in isotropic media," *IRE Trans. Antennas Propag.* **14**, 302–307 (1966).
15. H. Furukawa and S. Kawata, "Analysis of image formation in a near-field scanning optical microscope effects of multiple scattering," *Opt. Commun.* **132**, 170–178 (1996).
16. H. Furukawa and S. Kawata, "Local field enhancement with an apertureless near-field-microscope probe," *Opt. Commun.* **148**, 221–224 (1998).
17. A. Dunn, C. Smithpeter, A. J. Welch, and R. Richards-Kortum, "Finite-difference time-domain simulations of light scattering from single cells," *J. Biomed. Opt.* **2**, 262–266 (1997).
18. E. Evans and Y. Fung, "Improved measurement of the erythrocyte geometry," *Microvasc. Res.* **4**, 335–347 (1972).
19. S. C. Grover, R. C. Gauthier, and A. G. Skirtach, "Analysis of the behaviour of erythrocytes in an optical trapping system," *Opt. Express* **7**, 533–539 (2000).
20. J. D. Jackson, "Maxwell equations, macroscopic electromagnetism, conservation laws," Chap. 6 in *Classical Electrodynamics*, 3rd ed., pp. 258–262, John Wiley and Sons, New York (1999).
21. J. P. Gordon, "Radiation forces and momenta in dielectric media," *Phys. Rev. A* **8**, 14–21 (1973).
22. J. P. Berenger, "A perfectly matched layer for the absorption for electromagnetic waves," *J. Comput. Phys.* **114**, 185–200 (1994).
23. K. R. Umashankar and A. Taflove, "A novel method to analyze electromagnetic scattering of complex objects," *IEEE Trans. Electromagn. Compat.* **24**, 397–405 (1982).
24. A. Taflove, *Computational Electrodynamics: The Finite Different Time Domain Method*, Artech, Boston (1995).
25. Y. L. Xu, "Electromagnetic scattering by an aggregate of spheres," *Appl. Opt.* **34**, 4573–4588 (1995).